Aquatic Sciences (2022) 84:36
https://doi.org/10.1007/s00027-022-00867-2

Aquatic Sciences

RESEARCH ARTICLE

Hydrology influences carbon flux through metabolic pathways in the hypolimnion of a Mediterranean reservoir

J. J. Montes-Pérez[1] · R. Marcé[2,3] · B. Obrador[4,5] · T. Conejo-Orosa[1] · J. L. Díez[1] · C. Escot[6] · I. Reyes[6] · E. Moreno-Ostos[1]

Received: 16 January 2022 / Accepted: 5 April 2022

Abstract

Global change is modifying meteorological and hydrological factors that influence the thermal regime of water bodies. These modifications can lead to longer stratification periods with enlarged hypolimnetic anoxic periods, which can promote heterotrophic anaerobic processes and alter reservoir carbon cycling. Here, we quantified aerobic and anaerobic heterotrophic processes (aerobic respiration, denitrification, iron and manganese reduction, sulfate reduction, and methanogenesis) on dissolved inorganic carbon (DIC) production in the hypolimnion of a Mediterranean reservoir (El Gergal, Spain) under two contrasting hydrological conditions: a wet year with heavy direct rainfall and frequent water inputs from upstream reservoirs, and a dry year with scarce rainfall and negligible water inputs. During the wet year, water inputs and rainfall induced low water column thermal stability and earlier turnover. By contrast, thermal stratification was longer and more stable during the dry year. During wet conditions, we observed lower DIC accumulation in the hypolimnion, mainly due to weaker sulfate reduction and methanogenesis. By contrast, longer stratification during the dry year promoted higher hypolimnetic DIC accumulation, resulting from enhanced methanogenesis and sulfate reduction, thus increasing methane emissions and impairing reservoir water quality. Aerobic respiration, denitrification and metal reduction produced a similar amount of DIC in the hypolimnion during the two studied years. All in all, biological and geochemical (calcite dissolution) processes explained most of hypolimnetic DIC accumulation during stratification regardless of the hydrological conditions, but there is still ~ 30% of hypolimnetic DIC production that cannot be explained by the processes contemplated in this study and the assumptions made.

Keywords Thermal stratification length · Hypolimnion · Dissolved inorganic carbon · Metabolic rate · Sulfate reduction · Methanogenesis · Anoxia

Introduction

The role of inland waters in the global carbon cycle is disproportionately large in relation to the surface they occupy on Earth (Cole et al. 2007; Tranvik et al. 2009; Borges et al. 2015). Lakes and reservoirs represent an important long term carbon sink both at local and global scale (Kastowski et al. 2011; Dean and Gorham 1998; Kortelainen et al. 2004; Chmiel et al. 2016). These aquatic ecosystems bury carbon more efficiently than oceans due to higher sedimentation rates, lower oxygen exposition and larger and more frequent allochthonous (terrestrial) organic matter inputs (Sobek et al. 2009). In the case of reservoirs, carbon buried in their sediments constitutes around 40% of the total carbon sink in inland waters (Mendonça et al. 2017), a relevant value resulting from typically large catchments (Doubek and

✉ J. J. Montes-Pérez
jmontesp@uma.es

1 Department of Ecology and Geology, Marine Ecology and Limnology Research Group, Universidad de Málaga, Málaga, Spain

2 Catalan Institute for Water Research (ICRA), Girona, Spain

3 Universitat de Girona, Girona, Spain

4 Departament de Biologia Evolutiva, Ecologia i Ciències Ambientals, Facultat de Biologia, Universitat de Barcelona (UB), Av. Diagonal 643, 08028 Barcelona, Spain

5 Institut de Recerca de la Biodiversitat (IRBio), Universitat de Barcelona (UB), Barcelona, Spain

6 Empresa Metropolitana de Abastecimiento Y Saneamiento de Aguas de Sevilla (EMASESA), Seville, Spain

Published online: 16 May 2022

Carey, 2017) depicting high erosion rates (Anderson et al. 2020).

In the Mediterranean region, lakes and reservoirs usually show a warm monomictic thermal regime, characterized by a unique thermal stratification period that extends from spring to late fall (George 2010). During this thermally stratified period, the thermocline effectively isolates the hypolimnion, a net heterotrophic subsystem where both autochthonous and allochthonous organic matter is oxidized through diverse metabolic pathways. Once the thermocline is established, organic matter mineralization in the hypolimnion proceeds through aerobic respiration, using the limited hypolimnetic oxygen reserve as electron acceptor. The resulting oxygen depletion implies that organic matter oxidation must be carried out through anaerobic metabolic pathways, which depend on electron acceptors different from oxygen (e.g., nitrate, sulfate, manganic and ferric ions).

Anaerobic heterotrophic pathways are characterized by lower thermodynamic efficiency and rates of organic matter mineralization than aerobic respiration (Fenchel et al. 2012; LaRowe and Van Cappellen 2011). This has implications for the efficiency of organic carbon burial (Sobek et al. 2009). Therefore, anaerobic pathways play a crucial role in the carbon cycle in lake and reservoir ecosystems.

Thermal regime of lakes is influenced by hydrological and meteorological factors. Water inputs, withdrawals, precipitation and wind stress, among other factors, modify the stratification length and mixing frequency (Soares et al. 2019; Zhang et al. 2020; Liu et al. 2020). In addition, the onset of stratification is strongly related with hypolimnetic oxygen depletion, increasing the probability of anoxia with earlier thermocline development (Foley et al. 2012; Ladwig et al. 2021). In the present context of climate change, warming is increasing lake surface water temperature (Dokulil et al. 2021), which results in longer and more stable thermally stratified periods (Woolway et al. 2021; Butcher et al. 2015; Burns et al. 2005). Moreover, some ecosystems traditionally classified as warm monomictic are becoming permanently stratified (Woolway and Merchant 2019). Other global change pressures, such as catchment alterations, eutrophication, and decreasing fluvial inflows, also promote hypolimnetic anoxia (Marcé et al. 2010; Jenny et al. 2016).

In spite of the established fact that hydrological and meteorological future changes will impact thermal regimes, there is little information on carbon cycling in the hypolimnion under contrasting hydrological and meteorological conditions. Furthermore, although some studies have estimated the contributions of the main metabolic pathways (aerobic respiration, denitrification, iron and manganese reduction, sulfate reduction and methanogenesis) to DIC production in the hypolimnion, most research has been conducted in temperate lakes (Jones and Simon 1980; Schafran and Driscoll 1987; Kelly et al. 1988; Mattson and Likens 1993; Matthews et al. 2008; Fahrner et al. 2008), while studies in reservoirs are scarce (Wendt-Potthoff et al. 2014; McClure et al. 2021). In addition, none of these studies have quantified the contribution of each metabolic pathway to total respiration in the hypolimnion under contrasting hydrological conditions.

Climate change is expected to induce temperature increments and dryness in the Mediterranean region (IPCC 2021). As a consequence, Mediterranean reservoirs will show hydrological changes that will affect the quantitative and relative importance of different metabolic processes involved in hypolimnetic mineralization of organic matter.

In this paper, we used a mass balance approach to analyse carbon fluxes through diverse heterotrophic metabolic pathways (aerobic respiration, denitrification, sulfate reduction, Fe and Mn reduction and methanogenesis) and their contribution to DIC production in the hypolimnion of a Mediterranean reservoir during two thermally stratified periods with contrasting hydrological features. We expected that a longer stratification period during a dry year would enhance the role of anaerobic processes in the hypolimnetic respiration of organic matter. Conversely, we anticipated that water column instability and mixing during a wet year would lead to a shorter stratification period and a greater role of aerobic respiration in the hypolimnetic respiration of organic matter. We expect our results to be relevant for the adaptation of reservoir management practises to the already changing hydrological conditions as well as to anticipate potential alterations of carbon cycling in reservoirs.

Materials and methods

Study site

El Gergal (37º34′13"N; 6º02′57"E) is a Mediterranean reservoir located in South Iberian Peninsula (Seville, Spain). The reservoir has a surface of 250 ha, a capacity of 35 hm^3 and a maximum and mean depth of 37 m and 15.7 m, respectively. Water can be withdrawn from three different depths: via top (42.30 m.a.s.l), middle (26.35 m.a.s.l), and bottom outlets (18 m.a.s.l). This reservoir is the fifth in a cascade of five reservoirs in the Rivera de Huelva River. Water inputs come from the river, rainfall and runoff without any relevant groundwater input. All dams are used for water supply and the upstream dams, in addition, for downstream reservoir hydrological management, such as regulating input water, water residence time or water level. El Gergal is a mesotrophic reservoir with a warm monomictic thermal regime. The reservoir remains stratified a large part of the year, usually from spring to late fall (Cruz-Pizarro et al. 2005; Hoyer et al. 2009). Thermal stratification usually leads to oxygen depletion in the hypolimnion (Cruz-Pizarro et al. 2005).

Detailed information on hydrology (Moreno-Ostos et al. 2008; Moreno-Ostos et al. 2012), phytoplankton dynamics (Hoyer et al. 2009; Moreno-Ostos et al. 2009a, b; Rigosi and Rueda 2012), ecosystem metabolism (Moreno Ostos et al. 2016; Giling et al. 2017), and sedimentation processes (De Vicente et al. 2005) in El Gergal can be found elsewhere.

Sampling frequency and data collection

El Gergal reservoir was sampled biweekly during two whole thermally stratified periods (2018 and 2019). The 2018 stratification period started in May and finished in October, while the 2019 stratification period lasted from April to December.

During each survey, we used a 5 L Van Dorn bottle to collect water samples from four depths at the deepest point of the reservoir. In order to estimate diffusive flux of substances between the hypolimnion and the epilimnion, the first water sample was taken just above the thermocline. In the hypolimnion, three water samples were taken: below the oxycline, in the middle layer of the hypolimnion and 2–3 m above the sediment–water interface. Depths for sample collection were determined in situ after detailed analysis of a physico-chemical vertical profile (water temperature, dissolved oxygen concentration, pH, and water conductivity) collected from surface to bottom using YSI EXO2 multiparameter probe. A laboratory located on the shore of the reservoir was used to pre-process samples for subsequent analyses.

Chemical analyses

To determine SO_4^{2-}, NO_3^- and NH_4^+ concentrations, 50 mL water samples were in situ filtered through Whatman GF/C glass-fibre filters and stored frozen until analysis. Samples were analysed using ion chromatography (Metrohm "MODELO") with a high-performance separation column for the parallel determination of standard anions (Metrosep A Supp 7–250/4.0) and a column for cations (Metrosep C3-250/4.0).

For reduced metal ions (Fe^{2+} and Mn^{2+}) concentrations, 50 mL water samples were in situ filtered through Whatman GF/C glass-fibre filters and acidified with HNO_3 (1%). Filtered and acidified samples were analysed by ICP-MS (NexION 300D).

Methane concentration in water was measured using the headspace equilibrium technique and gas chromatography (Striegl et al. 2012). In order to avoid gas exchange with the atmosphere, 30 mL of water was directly taken on board, from the Van Dorn sampler using a syringe with stopcock and filled until 60 mL with ambient air. Additionally, one syringe was fill just with ambient air to calculate background CH_4 concentration. Syringes with stopcock were frequently shaken and kept at constant temperature in a water container during 30–60 min. Temperature was checked until the end of equilibrium and used to calculate Henry's coefficient between the liquid and the gas phase (Stumm and Morgan 1996). The equilibrated headspace was injected into 10 mL pre-evacuated glass vials (Agilent) and analysed using an Agilent 7820A gas chromatograph. Background CH_4 concentration was used to remove this effect from the equilibrium calculation.

CH_4 ebullitive flux was measured monthly following (Montes-Pérez et al. 2022). Gas bubbles were trapped using three inverted funnels equipped with a collector bottle. Bubble traps were deployed close to the dam in the lacustrine zone, and installed at 0.5 m depth. Once installed, bubble traps collected gas for 24 h. After this, collector bottles were gently screwed off and capped underwater. Then, collector bottles were weighted to calculate water volume displaced by gas bubbles. Gas was sampled from the collector through a rubber septum using a syringe and injected into 10 mL pre-evacuated glass vials (Agilent). In the laboratory, gas samples were analysed for CH_4 using an Agilent 7820A gas chromatograph.

Dissolved inorganic carbon

Dissolved inorganic carbon (DIC) concentration was determined from alkalinity and CO_2 concentration in water. Alkalinity was determined from 100 mL water samples acidified with HCl 0.01 N using automatic titration (Metrohm 808). For CO_2 concentration, 5 L water samples taken with the Van Dorn bottle were directly circulated through a gas transfer membrane contactor (Liqui-Cel™ MM Series) coupled to a portable CO_2 gas analyser (EGM-5 PP Systems) following Gómez-Gener et al. (2016). Readings of CO_2 in ppmv, CO_2 fugacity (fCO_2) were recorded every second until equilibrium was reached. Hyperbolic functions were fitted to the saturation curves to calculate fCO_2 in equilibrium. Partial pressure of CO_2 (ρCO_2) was calculated from fCO_2 and atmospheric pressure (P_{atm}):

$$\rho CO_2 = fCO_2 * P_{atm}$$

Then, CO_2 concentration in the water was calculated using the Henry's law:

$$\left[CO_2\right]_w = \rho CO_2 \cdot k_H$$

where k_H is the Henry's constant ($mol \cdot L^{-1} \cdot atm^{-1}$) estimated for in situ temperature and salinity (Zeebe and Wolf-Gladrow 2001; Weiss 1974; Millero 1995; Dickson and Goyet 1994).

Finally, DIC was calculated from $[CO_2]_w$, alkalinity, and water temperature and salinity using the R package AquaEnv (Hofmann et al. 2010).

Physical indices of the reservoir

We used rLakeAnalyzer R package (Winslow et al. 2019) to calculate physical indices of the reservoir. In order to introduce the effect of water level fluctuation on surface area and volume of column water layers, we modified `uStar()` and `schmidt.stability()` functions to calculated water friction velocity due to wind stress at the reservoir surface (m/s) and water column stability (Schmidt stability, J/m^2), respectively.

Volumetric metabolic rates

Volumetric metabolic rates were calculated from changes in the concentration of hypolimnetic substances implied in metabolic processes (Table 1). For each substance and thermally stratified period, a linear regression between concentration and time was fitted using the period during which each metabolic pathway was active. Concentration was averaged for the whole hypolimnion and corrected to account for vertical diffusive flux through the thermocline. Diffusive fluxes, J (mmol·m^{-2}·d^{-1}), were calculated for each chemical species as:

$$J = V_t \cdot \left(C_h - C_e\right)$$

where C_h and C_e are the mean concentrations in hypolimnion and epilimnion, respectively, for each sampling interval. In cases when samples taken above the thermocline were not clearly located within the epilimnion (because of a wider metalimnion), we used linear extrapolation to estimate concentration in the middle of epilimnion for DIC, NO_3^-, SO_4^{2-} and NH_4^+, while we assumed zero concentration for reduced manganese, iron, and methane in the epilimnion. To test that extrapolation was not introducing significant errors, we compared estimated concentration against actual concentrations obtaining p-values inferior than 0.05 ($n > 6$) for all substances. Thermocline heat transfer coefficient, V_t, was estimated following Chapra (1997) for each sampling interval:

$$V_t = \frac{V_h}{A_t t_s} ln \frac{\overline{T_e} - T_{h,i}}{\overline{T_e} - T_{h,s}}$$

where V_h and A_h are volume of hypolimnnion and contact surface area of hypolimnnion with epilimnion, respectively. V_h and A_h were calculated from the reservoir hypsographic curve and water level. T_e is the epilimnion averaged temperature and $T_{h,i}$ and $T_{h,s}$ are hypolimnion temperatures at the beginning and at the end for each calculation period. t_s is the interval time for which V_t is calculated. Top limit of hypolimnion was set at the thermocline. The position of the thermocline was calculated from temperature profiles as the depth of the maximum density gradient using the R package LakeAnalyzer (Winslow et al. 2019).

Changes in concentrations due to vertical diffusion flux (mmol·m^{-2}·d^{-1}) between two sampling days were calculated multiplying J by $A_h \cdot t_s$, and dividing by V_h to obtain changes in mmol·m^{-3}. Thus, corrected concentration in hypolimnion was calculated as:

$$C_{ch} = \overline{C_h} + \left(J \cdot \frac{A_h \cdot t_s}{V_h}\right)$$

Due to this correction, applied to include flux through thermocline, corrected concentration can show negative values when concentration in the hypolimnion is 0 (or close to 0) and a previous mass input through the thermocline has occurred.

Aerobic respiration was estimated from depletion of dissolved oxygen corrected concentration in the hypolimnion throughout the thermally stratified period. Anaerobic respiration was estimated from accumulation or depletion of chemical species involved in redox reactions throughout the stratification period. Electron acceptor consumption, SO_4^{2-} and NO_3^-, were used to estimate the magnitude of sulfate reduction and denitrification. Accumulation of reduced metal ions (Fe^{2+} and Mn^{2+}) and CH_4 was used to estimate organic matter oxidation by dissimilatory metal reducing bacteria (DMRB) and methanogenesis, respectively.

The contribution of the different metabolic pathways to total inorganic carbon production was estimated as the DIC

Table 1 Simplified redox reactions for each considered metabolic pathway in El Gergal reservoir hypolimnion

Metabolic pathway	Reaction	DIC equiv
Aerobic respiration	$\mathbf{O_2} + 4H^+ + 4e^- \rightarrow 2H_2O$	1
Denitrification	$\mathbf{NO_3^-} + 6H^+ + 5e^- \rightarrow 0.5N_2 + 3H_2O$	1.25
Manganese reduction	$2MnO_2 + 4H^+ + 4\,e^- \rightarrow 2\mathbf{Mn^{+2}} + 3H_2O$	0.5
Iron reduction	$4FeOOH + 8H^+ + 4\,e^- \rightarrow 4\mathbf{Fe^{+2}} + 7H_2O$	0.25
Sulfate reduction	$\mathbf{SO_4^{2-}} + 9H^+ + 8e^- \rightarrow HS^- + 4H_2O$	2
Methanogenesis	$CH_2O + 4H^+ + 4e^- \rightarrow \mathbf{CH_4} + H_2O$	1

Monitored substances are highlighted in bold in the redox equations. DIC equivalents produced per mol of substance

equivalents produced by every metabolic pathway following the redox reactions in table (Table 1) extracted from (Stumm and Morgan 1996; del Giorgio and Williams 2005a, b). Rates were multiplied by the number of days during which each metabolic process was active (activity period). For each studied metabolic pathway, the activity period was considered as the time period since a concentration change (accumulation or depletion) in the monitored redox substance was first noticed until the date when concentration change ends.

Estimated DIC

We calculated the DIC production in the hypolimnion considering two main processes: biological processes and geochemical processes (abiotic increase of alkalinity).

Biological DIC production was estimated as the sum of each volumetric metabolic rate multiplied by the number of active days. Geochemical processes, such as cation exchange and weathering, which affect alkalinity can also produce an increase of DIC. Alkalinity produced by abiotic processes during stratification was calculated by removing ions produced by metabolic pathways from the measured alkalinity increase:

$$Alk_{abiotic} = Alk_{measured_0} + \Delta Alk_{measured} - \Delta Alk_{biotic}$$

where $Alk_{measured0}$ is alkalinity measured at the beginning of stratification period and ΔAlk_{biotic} was defined as follows:

$$\Delta Alk_{biotic} = \Delta NH_4^+ - \Delta SO_4^{-2} - \Delta NO_3^-$$

The abiotic increase of alkalinity was used to estimate DIC production by geochemical processes by fitting a linear regression between abiotic alkalinity and time. The slope of the regression was multiplied by days of stratification to obtain a rate of alkalinity increase. From this, DIC production by geochemical processes in the hypolimnion was derived from the stoichiometry between carbonate dissolution (i.e. alkalinity increase) and DIC production. We assumed that an increase of alkalinity of 2 mol would produce 1 mol of DIC.

Results

Hydrology

The two studied years showed contrasting hydrological conditions. Stratification length was shorter during 2018 with a later onset of thermocline and an earlier fall turnover, two months earlier than in 2019 (Fig. 1).

Rainfall difference was remarkable, showing a clearly wet year with 730 mm rainfall in 2018, above the historical average of 500 mm for the area. By contrast, 2019 was a particularly dry year with rainfall below 300 mm. In addition, rainfall after summer started earlier and with greater

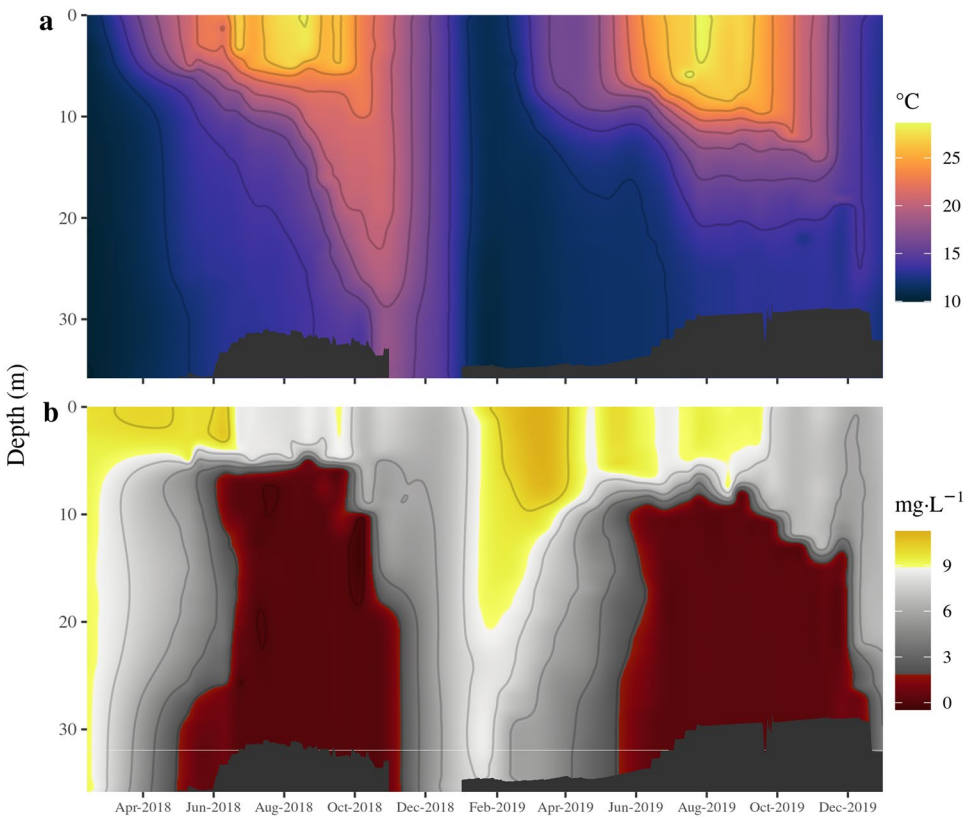

Fig. 1 Vertical profiles of temperature (**a**) and dissolved oxygen concentration (**b**) during the two studied years. Palette colour chosen from 'cmocean' R package (Thyng 2016)

intensity in 2018, whereas in 2019 fall precipitation was negligible (Fig. 2a). Water friction velocity due to wind stress at the reservoir surface was similar during both years with highest peaks related to storm events when precipitations were intense (Fig. 2b).

The hypolimnion remained thermally stable with a slight increase of temperature during stratification during both years. However, the epilimnion was thinner with a shallower thermocline in 2018 (6 m depth) than in 2019 (10 m depth). Thus, hypolimnetic volume was greater in 2018 than in 2019 (Table 2).

Reservoir management during 2018 introduced water from upstream reservoirs (Cala and Minilla reservoirs), whereas during 2019, water inputs were rather scarce (Fig. 2b). Furthermore, water withdrawals were higher during 2018. Therefore, mean water residence time during thermal stratification was much longer in 2019 (475 days) than in 2018 (162 days) (Table 2).

Water column stability increased throughout the stratification period, reaching highest stability between late July and August (Fig. 2b). However, during 2018, a bigger drop of stability was observed, a pattern that was not recorded in 2019, with November mean Schmidt stability above 100 $J \cdot m^{-2}$. In addition, reservoir water volume changes were apparent during 2018 (Fig. 2b), whereas in 2019, changes in reservoir water volume were minor.

Temporal dynamics of substances involved in redox reactions

Once thermal stratification was established, the hypolimnion was still well oxygenated. Mean oxygen concentration in the hypolimnion at the beginning of stratification was 103 ± 69 $mmol \cdot m^{-3}$ in 2018 and 133 ± 27 $mmol \cdot m^{-3}$ in 2019. During both years, oxygen was consumed quickly, reaching anoxia in the whole hypolimnion during the first weeks of July. From this moment on, oxygen trend was

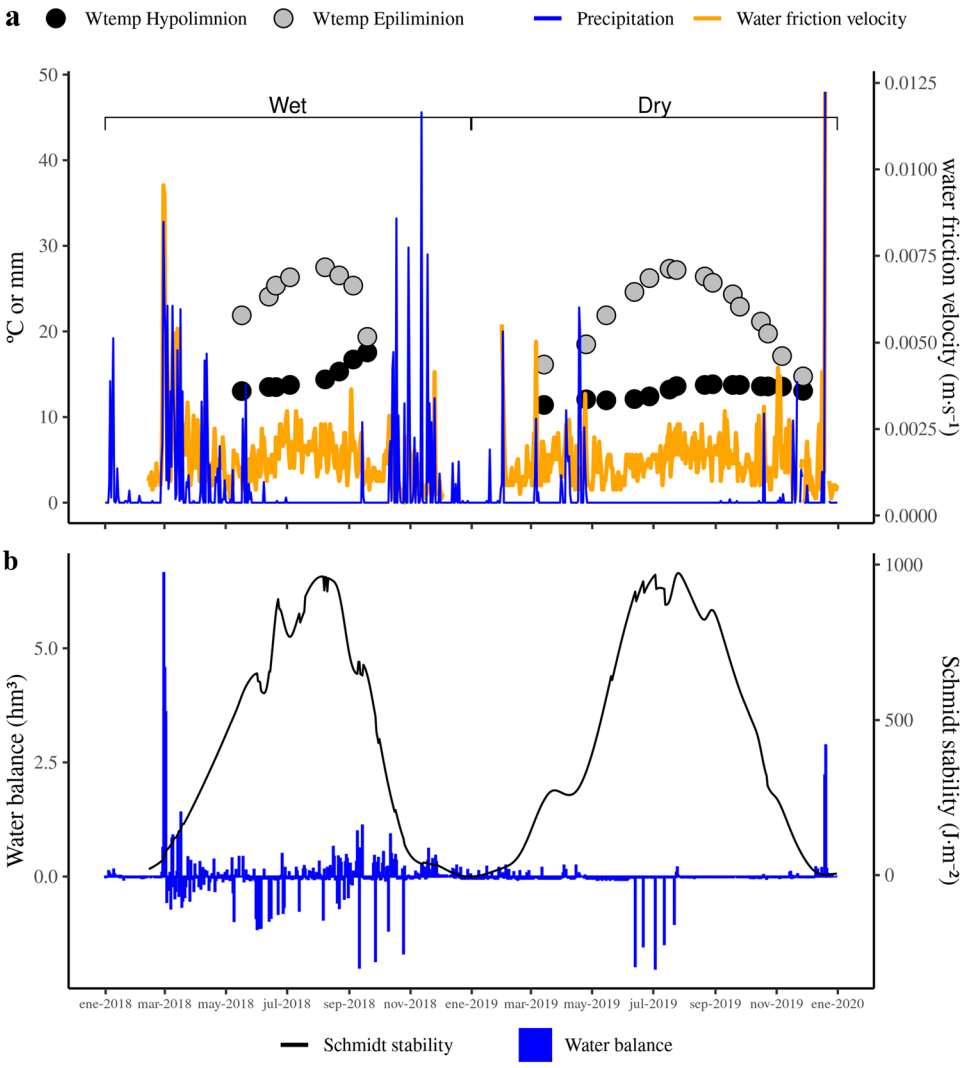

Fig. 2 Meteorological and hydrological conditions during the two studied years. **a** Precipitation is expressed in mm; Wtemp epilimnion/hypolimnion is the averaged water temperature for the whole layer in degrees Celsius; Water friction velocity due to wind stress in $m \cdot s^{-1}$. b Schmidt stability in ($J \cdot m^{-2}$); Dialy water balance in the reservoir (inlet water–outlet water). Meteorological data from *Red de Información Agroclimática de Andalucía*, https://www.juntadeandalucia.es/agriculturaypesca/ifapa/riaweb/web/

Table 2 Hydrological and limnological variables for the two studied stratification periods

	Units	2018	2019
Stratification	Days	157 (01-May—> 10-Oct)	279 (01-April—> 05-Dec)
Water level	masl	47.05 (50.06-46.68)	45.92 (49.15-43.34)
Thermocline depth (start–end)	m	6 (5–12)	10 (9–19)
Total volume (start–end)	hm^3	27.7 (35.0-28.1)	26.06 (32.6-20.4)
Hypolimnion volume	hm^3	19.28	12.25
Total water input	hm^3	27.84	2.99
Total water output	hm^3	25.28	7.197
Hypolimnion water residence time	Days	162	475
Tmax air	ºC	31.48	28.61
Te	ºC	24.55	22.26
Th	ºC	15.51	13.70
Rain	mm	731	238
Chl-a	$\mu g \cdot L^{-1}$	8.3	6.4

Average values and values at the beginning and at the end of stratification (in brackets). Meteorological data from *Red de Información Agroclimática de Andalucía*, https://www.juntadeandalucia.es/agriculturaypesca/ifapa/riaweb/web/

roughly constant with a slight decrease because of vertical diffusion flux which introduced small amounts of oxygen in the hypolimnion during anoxia (Fig. 3a).

NO_3^- concentration showed a decrease after the onset of thermocline, when oxygen was still not completely depleted in the hypolimnion (Fig. 3b). NO_3^- mean concentration increased slightly at the very beginning of stratification, reaching its maximum concentration few weeks later, 44.3 ± 5 mmol·m^{-3} in 2018 and 43.4 ± 7.6 mmol·m^{-3} in 2019. After this maximum, NO_3^- mean concentration decreased at the end of June in 2018, whereas in 2019, denitrification began earlier, at the end of May. In 2018, NO_3^- reached minimum mean concentration in the hypolimnion in September (8 ± 3.1 mmol·m^{-3}), while in 2019, NO_3^- was completely depleted at the middle of August (0.7 ± 0.1 mmol·m^{-3}).

Reduced manganese accumulation began when oxygen was almost depleted, at the end of June during both years, and concentration increased until the end of the stratification, reaching maximum values of 9.2 ± 5.6 mmol·m^{-3} (September 2018) and 11.9 ± 4.3 mmol·m^{-3} (November 2019) (Fig. 3d). In its turn, reduced iron accumulation began well before reduced manganese accumulation in 2018, while reduced iron accumulation did not begin until the end of July in 2019 (Fig. 3c). Maximum reduced iron mean concentration in the hypolimnion was recorded at the end of stratification, in September 2018 (6 ± 5.5 mmol·m^{-3}) and November 2019 (13.7 ± 0.7 mmol·m^{-3}).

Decrease of sulfate concentrations was evident throughout the whole stratification period (Fig. 3e). From the first survey to the last, mean sulfate concentration in the hypolimnion decreased from 115.5 ± 14.8 to 71.7 ± 7.8 mmol·m^{-3} in 2018, and from 188.5 ± 10.8 to 106.6 ± 7.8 mmol·m^{-3} in 2019.

In 2018, methane accumulation in the hypolimnion was low, reaching a mean concentration of 8.16 ± 5.6 mmol·m^{-3}. In contrast, in 2019, methane accumulation started in September and reached up to 53.6 ± 45.6 mmol·m^{-3} before fall turnover (Fig. 3f).

Ammonium accumulation became apparent when oxygen was completely depleted, and reached its maximum concentration before fall turnover, 15.4 ± 5.6 mmol·m^{-3} in 2018 and 55.6 ± 42 mmol·m^{-3} in 2019 (Fig. 3g).

DIC concentration was slightly lower during 2018 than in 2019 (Fig. 3h). Nonetheless, DIC concentration increased constantly throughout the stratification period during both years, until 1805 ± 91 mmol·m^{-3} in 2018 and 2584 ± 154 mmol·m^{-3} in 2019.

Vertical heat transfer during the stratification period ranged from 0.01 to 0.066 m·d^{-1} with a mean value of 0.03 m·d^{-1} in 2018 and 0.001–0.05 m·d^{-1} with a mean value of 0.016 m·d^{-1} in 2019. The effect of vertical diffusion through the thermocline did not imply significant changes in redox substances concentrations during the studied stratification periods (Supplementary material).

Methane ebullitive flux accounted for a very small proportion (< 1%) of the DIC produced and was not included in subsequent calculations.

Metabolic rates

Consumption and accumulation of redox substances followed similar patterns in both years (Fig. 3). However, metabolic rates and their activity period changed from

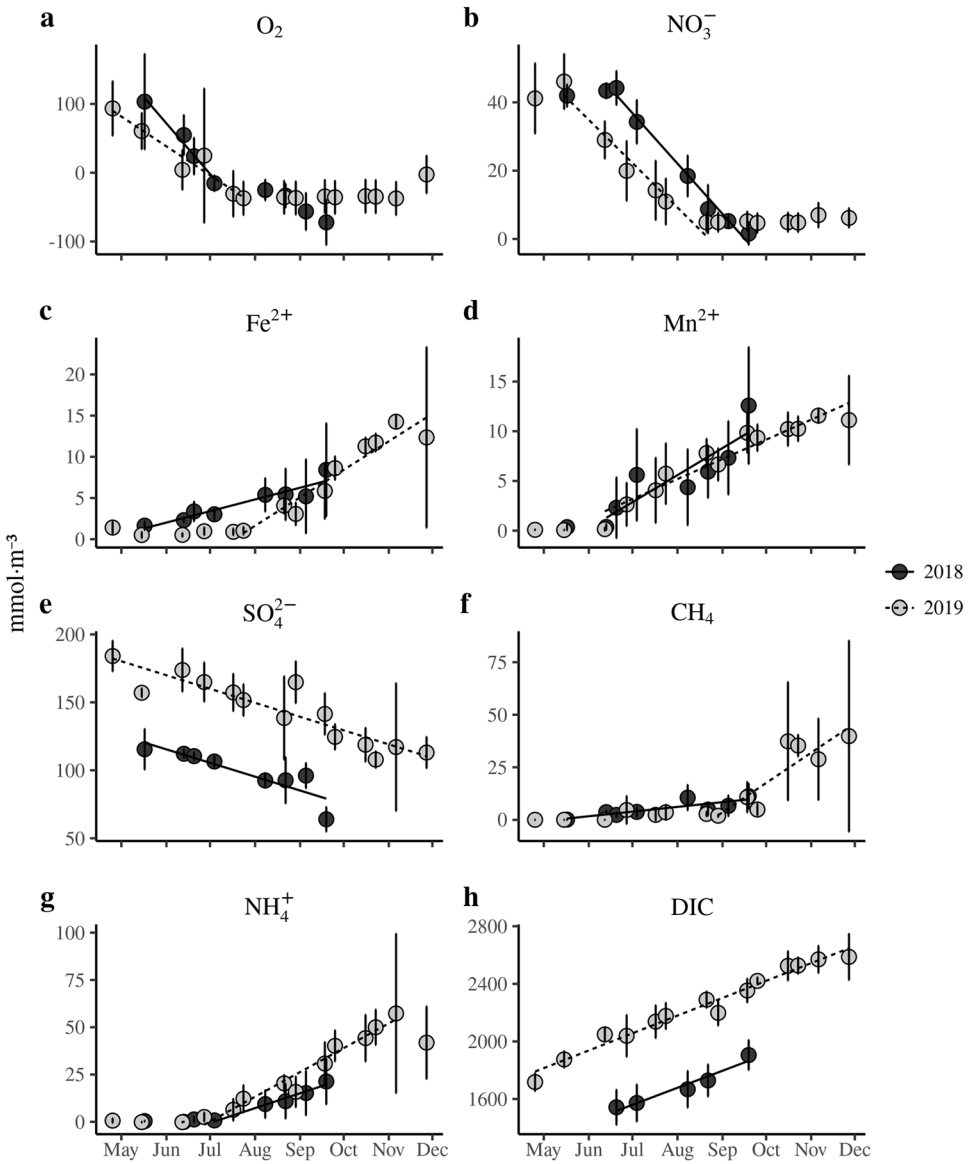

Fig. 3 Mean concentration in the hypolimnion of "El Gergal" reservoir during both studied years, 2018 (black points) and 2019 (grey points). Concentration is corrected with vertical diffusion flux. Vertical bars depict standard deviation and lines are linear regression for 2018 (solid line) and 2019 (dashed line)

2018 to 2019. Aerobic respiration, iron reduction and methanogenesis showed the largest differences (Table 3).

DIC accumulation rates were similar during both years (Table 3). Nonetheless, total DIC accumulated during the stratification period was higher in 2019 because activity period lasted 216 days, whereas in 2018, activity period lasted 125 days. Likewise, sulfate reduction depicted the highest rates of anaerobic metabolism with similar rates in both years, and it was active throughout the entire stratification period; therefore, active time was 125 days in 2018 and 216 days in 2019.

Table 3 Rates, expressed as DIC equivalents, estimated from linear regression for each metabolic pathway and geochemical processes

Year	Rates mmol DICeq·m^{-3}·d^{-1}							
	DIC_m	O_2	NO_3^-	Fe	Mn	SO_4^{2-}	CH_4	DIC_{geo}
2018	3.82	2.45	0.60	0.01	0.04	0.66	0.07	0.48
2019	3.97	1.40	0.53	0.03	0.03	0.66	0.46	0.88

DIC_m is rate from DIC measured in the hypolimnion, *O_2* aerobic respiration, *NO_3^-* denitrification, *Fe* iron reduction, *Mn* manganese reduction, *SO_4^{2-}* sulfate reduction, *CH_4* methanogenesis, *DIC_{geo} DIC* produced by geochemical processes

Aerobic respiration was the highest metabolic pathway during both stratification periods, with rates and active times markedly different between years. In 2018, oxygen was consumed faster (2.45 $mmol \cdot m^{-3} \cdot d^{-1}$) but activity period was shorter (48 days) than in 2019, when aerobic respiration rate was 1.4 $mmol \cdot m^{-3} \cdot d^{-1}$ and lasted 90 days. In contrast to aerobic respiration, denitrification rates were similar during 2018 and 2019 and showed the same activity period, around 90 days (Table 3).

Metals reduction (Fe and Mn) depicted the lowest rates of all studied metabolic pathways (Table 3). Despite iron reduction starting later in 2019, rates were active for the same length of time. Iron reduction rate was lower in 2018. On the contrary, manganese reduction showed similar rates, but depicted a longer activity period in 2019.

Methanogenesis rates showed the highest differences between years, with a rate sevenfold higher and lower active time in 2019. Methanogenesis shifted from being one of the lowest metabolic rates in 2018 to reach a rate similar to sulfate reduction and denitrification in 2019. In the latter case, methanogenesis was more intense and constrained to the last period of stratification, whereas in 2018, methane accumulation was slow but continuous throughout the whole stratification period.

DIC production by geochemical processes was more intense in 2019 than in 2018 (Table 3; Fig. 4).

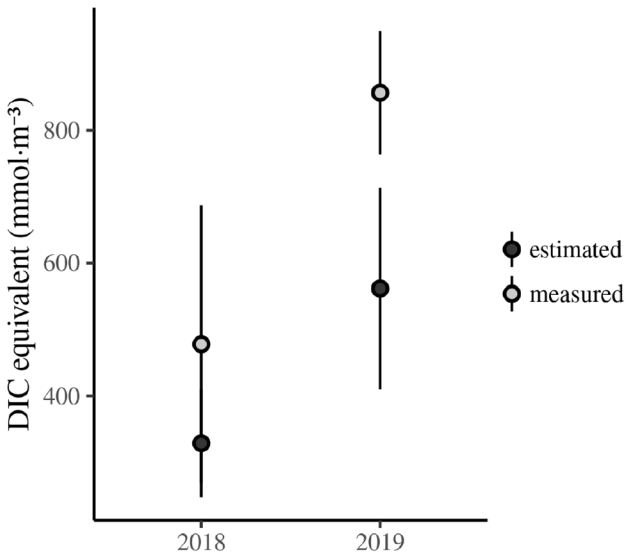

Fig. 5 DIC equivalent produced during the stratification period for each year. Black points are estimated DIC from metabolic pathways production and geochemical processes. Grey points are measured DIC calculated from actual measures of DIC concentration in the hypolimnion. Points are mean values and vertical lines depict standard deviation

Sources of DIC

DIC accumulation during the 2018 stratification period (478, 95% CI [269, 687] $mmol \cdot m^{-3}$) was markedly lower that DIC accumulation during 2019 (857 [764, 950] $mmol \cdot m^{-3}$) (Fig. 5). In addition, the DIC produced by metabolic processes was lower in 2018 (269 [192, 346] $mmol \cdot m^{-3}$), than in 2019 (372 [301, 443] $mmol \cdot m^{-3}$) (Fig. 6a). The difference between DIC produced by biological processes in 2018 and 2019 was related to the metabolic processes with the lowest energy yield, sulfate reduction and methanogenesis. In 2019, sulfate reduction produced 60 $mmol \cdot m^{-3}$ DIC more than in 2018. CH_4 production increased 30 $mmol \cdot m^3$ in 2019 compared with CH_4 produced during 2018. Conversely, the amount of DIC produced by the thermodynamically more favourable metabolic processes was similar during the two years, around 120 $mmol \cdot m^{-3}$ for aerobic respiration and 50 $mmol \cdot m^{-3}$ for denitrification (Fig. 6a). DIC produced by DMRB was slightly higher in 2019.

Biological processes produced 82% of DIC in 2018, whereas in 2019, their contribution dropped to 66% (Fig. 6b). Although aerobic respiration stopped contributing to the total hypolimnetic DIC production in July, at the end of both studied stratification periods, it was the most relevant

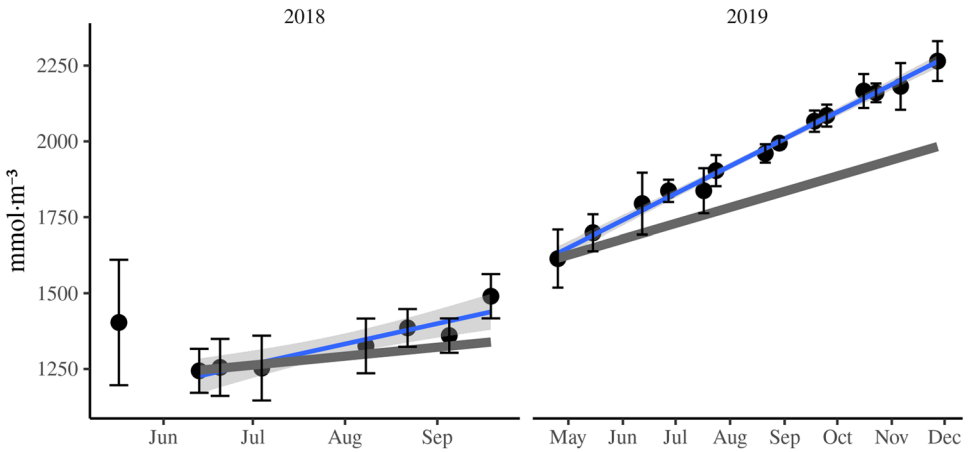

Fig. 4 Abiotic alkalinity increment in the hypolimnion of "El Gergal" reservoir during both studied years, 2018 (**a**) and 2019 (**b**). Points are mean values and vertical lines depict standard deviation of measured alkalinity. Gray line show linear increase in alkalinity due to abiotic factors. Blue line shows linear fit and the grey region represents the confidence interval

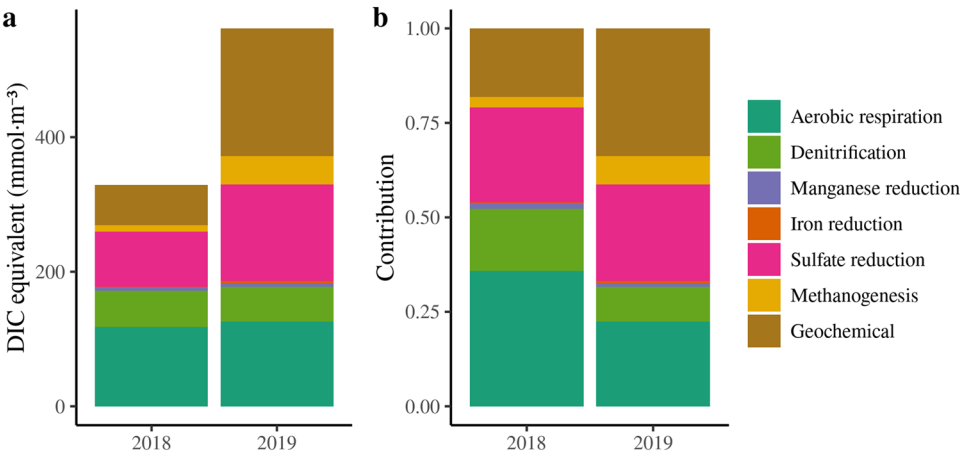

Fig. 6 **a** Production and **b** relative contribution of each considered metabolic pathway and geochemical processes in the total DIC generated during stratification, expressed as DIC equivalent

metabolic pathway in terms of DIC production. Aerobic respiration and denitrification contributions were higher in 2018 (Fig. 6b). On the contrary, methane contribution was higher during the longest stratification period (2019), 7% instead of 3% in 2018 (Fig. 6b). Sulfate reduction was the main anaerobic pathway in terms of DIC equivalent production contributing ~ 25% of estimated DIC in both years (Fig. 6b). Contribution of DMRB was low, accounting for 1% to estimated DIC in the hypolimnion (Fig. 6b).

DIC produced by geochemical processes was roughly two-fold lower in 2018 than in 2019 (60 [18, 102] and 190 [162, 218] mmol·m^{-3}, respectively) (Fig. 6a). Furthermore, geochemical contribution to estimated DIC in 2018 (18%) was lower than in 2019, when it reached 33% of DIC produced.

Finally, the sum of DIC produced by biological and geochemical processes seems to underestimate total measured DIC in the hypolimnion during both stratification periods (Fig. 5). Estimated DIC from biological and geochemical processes supposed around 70% of DIC measured in the hypolimnion both years. Thus, there is a 30% of measured DIC which cannot be explained by the processes and assumptions considered in this study.

Discussion

Overall, our expectation that a longer stratification period during dry years would enhance the role of anaerobic processes in the hypolimnetic respiration of organic matter was sustained by our analysis. The amount of aerobic respiration during the two years was nearly identical, but several alternative sources of DIC increased during the dry year (Fig. 6). This was mostly consistent in an increase in sulfate reduction and the geochemical production of DIC, and to a lesser extent, methanogenesis. This implies that aerobic respiration depicts a smaller relative contribution to DIC production during dry years compared to wet years.

Dynamics and contribution to DIC by metabolic pathways non-limited by the availability of electron acceptors

In El Gergal reservoir, it seems there is no limitation by electron acceptors or organic matter availability for some anaerobic processes (iron and manganese reduction, sulfate reduction and methanogenesis), because these substances keep changing until the end of stratification regardless of the duration of the stratification period (Fig. 3). For other substances (oxygen, nitrate), the electron acceptors completely deplete before the end of stratification.

DIC and methane accumulated in the hypolimnion were higher when the stratification period was lengthened (Fig. 3). Although a similar trend in hypolimnion metabolic pathway succession was observed during these two contrasting stratification periods, the activity period of each route changed. This is more conspicuous for the less thermodynamically advantageous metabolisms, such as methanogenesis and sulfate reduction. These anaerobic processes were active until the end of stratification showing a longer activity period in 2019. Nonetheless, if instead of an anoxic hypolimnion a well oxygenated water column prevailed during the same period, DIC production could be increased. It is well known that aerobic respiration is more efficient than anaerobic alternative heterotrophic pathways, and it will produce more CO_2 (Carey et al. 2018; LaRowe and Van Cappellen 2011). However, previous studies (Huttunen et al. 2001; Hounshell et al. 2021) have revealed that CO_2 production can be similar under oxic and anoxic conditions. In this study, DIC production does not change during any stratification period when oxic-anoxic transition took place, which could suggest similar CO_2 production under oxic and anoxic conditions. This is not the case

for methanogenesis. A longer stratification period leads to the depletion of the more thermodynamically favourable electron acceptors, such as oxygen and nitrate. Meanwhile, methanogenesis can be active for longer, generating more methane. In addition, a deepening of the thermocline during early fall can promote phytoplankton production (Cantin et al. 2011; Giling et al. 2017) and, thus, increase organic matter settling flux (Simola 1981; Wetzel 2001; Carpenter et al. 1986). Primary production peaks could enhance methane production rates during late summer and autumn, promoting a higher methane production than expected when stratification is extended. A fraction of this accumulated methane will release to the atmosphere during the fall turnover (Montes-Pérez et al. 2022; Vachon et al. 2019; Encinas-Fernández et al. 2014).

Although temporal dynamics of the studied redox substance concentrations followed the expected sequence according to energy yield, sulfate reduction was active from the onset of thermal stratification. In El Gergal reservoir, sulfate reduction seems to be active from the onset of stratification in both years, even when oxygen is still available. During these aerobic early stages, sulfate reduction could take place close to the sediment, depleting sulfate from the hypolimnion. Moreover, sulfate reduction showed activity during the whole stratification period, reaching the lowest sulfate concentrations around 60–100 µM, which are not limiting concentrations for sulfate-reducing bacteria in limnetic environments (Holmer and Storkholm 2001), indicating that sulfate reduction could be active even longer.

Metal reductions did not play a significant role in total DIC production (< 1% of DIC produced by m^3). However, both Mn and Fe metabolisms produced more DIC during the longest stratification period than in the shortest one. Manganese reduction showed similar rates both years, but the longer anoxia period led to higher DIC production at the end of the stratification. In the case of Fe reduction, it can be active in the anoxic sediment before anoxia reaches the whole hypolimnion. In 2018, we could measure this activity during the early stage of stratification due to heterogeneous hypolimnion which could hold anoxic conditions in the deepest layers. The lower Fe reduction rate could be due to the effect of Fe^{2+} oxidation in that heterogeneous hypolimnion. On the other hand, in 2019, hypolimnion was more homogeneous and, therefore, Fe reduction activity is noticed later than in 2018 and depicts a higher rate because of the smaller Fe^{2+} oxidation effect. In addition, Balistrieri et al. (1992) reported that Fe^{2+} accumulated in the hypolimnion of Sammamish lake was produced by releasing from sediment and reduction of Fe oxide particles settling through anoxic water column. This Fe reduction in the water column could also lead to the higher rate recorded during 2019.

Dynamics and contribution to DIC by metabolic pathways limited by the availability of electron accept

Aerobic respiration and denitrification ceased their activity during stratification due to electron acceptors limitation both studied years. Actually, during the longest stratification period (2019), production of DIC by anaerobic metabolism was higher, except for denitrification (Fig. 6). Denitrification was the only anaerobic pathway which had limited activity due to NO_3^- depletion (Fig. 3). Thus, this route showed quite similar rates and activity periods between years, with just a small delay due to the onset of thermal stratification. DIC production by aerobic respiration and denitrification were similar both years. This could be the result of complete electron acceptors (oxygen and nitrate) depletion during the thermally stratified period. In a variety of aquatic ecosystem, it has been demonstrated that denitrification is mainly limited by NO_3^- availability (Megonigal et al. 2014; Lohse et al. 1993; Nowicki 1994) and oxygen respiration is linear until oxygen is almost depleted (del Giorgio and Williams 2005b; Cornett and Rigler 1984). Therefore, total DIC produced through these pathways is determined by the availability of electron acceptors at the moment of hypolimnion isolation.

Furthermore, aerobic respiration rate was higher in 2018, within the range reported by Cornett and Rigler (1984) for several lakes. This higher rate can be related to a peak of chlorophyll found during late spring in the epilimnion, reaching values of 12.7 y 7.1 $\mu g \cdot L^{-1}$ in May and June, respectively. This biomass peak could result in an increased epilimnetic organic matter flux to hypolimnion (Baines et al. 1994). Actually, permanganate index, which is related to organic matter content, showed a higher value in the hypolimnion during that period (6.10 ± 0.49 $mg \cdot L^{-1}$) than in 2019 (3.84 ± 0.25 $mg \cdot L^{-1}$). Increased primary production has been previously related to oxygen consumption in hypolimnion (Yuan and Jones, 2020; Edwards et al., 2005). Although this biomass peak leads to a faster hypolimnetic oxygen consumption, total amount (mmol) of respirated oxygen by cubic meter depends on the oxygen available at the onset of hypolimnion isolation. Initial hypolimnetic oxygen concentration was similar in both years, being mostly related to water temperature and stratification timing.

It should be noticed that sediment reached anoxia before the water column and, consequently, anaerobic metabolism began earlier in the sediment. Reduced compounds released by anaerobic respiration (Fe^{2+}, Mn^{2+}, HS^-) can consume an important amount of oxygen (Müller et al. 2012). Therefore, aerobic heterotrophic respiration could be overestimated. Nevertheless, oxygen consumption by oxidation of reduced compounds would result in the same ratio of O_2 consumed:DIC produced than aerobic respiration. This is because the amount of oxygen consumed to produce 1 mol

of CO_2 by aerobic respiration is the same as the amount of oxygen consumed by oxidation of reduced substances whose production releases 1 mol of CO_2 (Gelda et al. 1995; Müller et al. 2012). Thus, this could slightly change the contribution of each metabolic pathway to estimated DIC, but estimated DIC would be the same. However, aerobic oxidation of methane is an exception because it consumes more oxygen (2 mol) to oxide 1 mol of CH_4 for which 1 mol of DIC was produced. In this case, estimated DIC would be lower than expected here and difference with measured DIC would be higher.

Unexplained DIC sources

DIC production by metabolic processes and geochemical processes cannot fully explain DIC changes in the hypolimnion of El Gergal reservoir (Fig. 5). In El Gergal reservoir, geochemical processes can play a relevant role in DIC production during thermal stratification, accounting for around 10–20% of total measured DIC. Schindler et al. (1986) found that around 40% of generated alkalinity in Lake 239 was abiotic, meanwhile 60% resulted from biotic processes (sulfate reduction and denitrification mainly). In El Gergal, limited water input during 2019 together with an increase of alkalinity suggest an internal source of DIC. The most important abiotic processes which can generate alkalinity and DIC are $CaCO_3$ and $MgCO_3$ dissolution. Magnesium concentration did not change during any of the studied years, whereas calcium increased its concentration (data not shown). Ca^{2+} increase could result from dissolution of sedimentary calcite or from dissolution of calcite settling from the epilimnion. Nevertheless, an increase of Ca^{2+} was recorded in the hypolimnion, especially during 2019 (around 40 $mmol \cdot m^{-3}$). This Ca^{2+} increase came from calcite dissolution could account for around 22% of geochemical DIC increase. Thus, there is still a lack of DIC source which cannot be explained by calcite dissolution nor any of the considered metabolic pathways. Information available from this study did not allow to unravel these sources of DIC.

In other studies (Yi et al. 2021; Wang et al. 2020), river inflow can increase DIC concentration in the reservoir with a karstic watershed. However, this is not the case for El Gergal which is located in a siliceous region. Besides, the inflow effect should result in a greater unbalance in 2018 than in 2019 because of negligible water inflow during the last year. Although during 2018, C input from the river could be plausible, these inflows were not continuous and we should have noticed an abrupt DIC increase. By contrast, DIC concentration showed a smooth and continuous increase during the whole stratification period. In addition, water temperature of the inflow water and reservoir water would have implied river insertion depth at the level of the epilimnion. Therefore, any external DIC load would not have directly affected the hypolimnion.

Ferrous ion and sulfide can precipitate reducing Fe^{2+} accumulation in the water column. Unfortunately, there are no sediment data on ferrous sulfide accumulation in El Gergal. However, sulfate reduction was estimated from depletion. Therefore, only DIC produced by iron reduction could be underestimated. In any case, just a fraction of DIC produced by the iron reduction pathway could be missed from our calculations due to ferrous sulfide precipitation. Furthermore, iron reduction contribution to total DIC is expected to be low since in similar studies, iron reduction usually represents less than 5% of total DIC produced (Table 4). Consequently, this process is not expected to account for a relevant amount of DIC.

Implications of using volumetric vs. areal rates for interpretation of metabolism

Metabolic processes can take place in sediments as well as in the water column, both affecting DIC production in the hypolimnion. Both volumetric rates and areal rates present limitations in interpreting results. The former will capture differences between metabolic processes which take place mainly in the water column. Meanwhile, the latter can capture differences between processes taking place mainly in sediments. The same volumetric rate of a metabolic process with higher activity in the water column will result in different areal rates if the hypolimnion volume and surface area of thermocline ratio (V_h/A_{ther}) is different. On the other hand, a different V_h/A_{ther} ratio will not affect two similar areal rates of processes mainly active in sediments. Meanwhile, these two similar areal rates could result in different volumetric rates if there is different hypolimnion volume. In both cases, changes in organic matter oxidation rates could be masked by hypolimnion volume changes. This can be a minor issue in lakes where water level fluctuation is negligible, but reservoirs with typically high water level fluctuation can represent significant changes.

In this study, denitrification and sulfate reduction volumetric rates showed similar values in both years (Table 3), whereas marked differences appeared in terms of areal rates (Table 4). This could suggest a relevant role of water column in DIC production through these metabolic pathways, which have been widely reported (Eckert and Conrad 2007; Beaulieu et al. 2014; Karnachuk et al. 2006; Grantz et al. 2012). The case of manganese reduction appears to be the opposite, differences are smaller when rates are expressed as areal rates, which might indicate a similar rate of manganese reduction in sediments both years. The differences become more evident when rates are expressed in volumetric rates and hypolimnion volume is quite different. Iron reduction and methanogenesis showed differences even when rates are

Table 4 Comparison of areal hypolimnetic DIC production rates by different metabolic pathways in freshwater ecosystems

Lake	DIC measured	O_2	NO_3^-	Fe	Mn	SO_4^{2-}	CH_4	References
Blelham tarn	10.7	4.49 (42)	1.46 (17)	0 (0)	NA	0.1 (2)	2.68 (25)	Jones and Simons (1980)
Dart's	4.7	3.81 (81)	0.56 (15)	0.04 (0.2)	0.02 (0.16)	0.08 (4)	0 (0)	Schafran and Driscoll (1987)
L226	8.1	3.81 (47)	0.84 (13)	0.97 (3)	0.14 (0.88)	0.9 (25)	5.75 (71)	Kelly et al. (1988)
L227	7.38	0.41 (5.5)	0.06 (1)	0.59 (2)	0.04 (0.29)	0.98 (30)	5.02 (68)	
L223	7.62	0.69 (9)	0.06 (1)	1.83 (6)	0.13 (0.86)	1.02 (30)	3.2 (42)	
Mirror	5.33	2.29 (43)	0 (0)	0.43 (2)	NA	0.17 (7)	0.59 (11)	Mattson and Likens (1993)
Meerfelder maar	16	3.52 (22)	0.51 (4)	0.32 (0.5)	NA	1.12 (14)	8.96 (56)	Fahrner et al. (2008)
Onondaga	51.9	14.53 (28)	3.74 (9)	2.08 (1)	NA	11.42 (44)	9.86 (19)	Matthews et al. (2008)
Hassel	4.4	5.94 (135)	3.8 (108)	0.35 (2)	0.63 (7.2)	2.66 (121)	1.76 (40)	Wendt-Potthoff et al. (2014)
Rappbode	8.6	3.35 (39)	0.62 (9)	0.52 (1.51)	0.74 (4.3)	1.2 (28)	1.29 (15)	
Beaverdam Reservoir	2.6	0.19 (7.4)	0 (0)	0.47 (18)	0.08 (3)	0.07 (2.6)	1.79 (69)	McClure et al. (2021)
Gergal 2018	44.93	28.79 (64.09)	6.99 (15.56)	0.14 (0.3)	0.52 (1.15)	7.74 (17.22)	0.86 (1.91)	This study
Gergal 2019	40.81	14.38 (35.25)	5.42 (13.27)	0.29(0.7)	0.33 (0.82)	6.84 (16.76)	4.78 (11.72)	

Rates expressed in $mmol \cdot m^{-2} \cdot d^{-1}$. In brackets, the percentage of DIC accumulated. *NA* not available

O_2 aerobic respiration, NO_3^- denitrification, *Fe* iron reduction, *Mn* manganese reduction, SO_4^{2-} sulfate reduction, CH_4 methanogenesis

shown as areal rates (Fig. 4). Thus, if these processes are mainly confined to sediments (Bastviken et al. 2008, 2011; Canfield et al. 2005; Peeters et al. 2019), it is possible that higher rates in 2019 are not only due to a lower hypolimnetic volume but also would result from increased metabolic rates in sediments. These higher rates in 2019 could be influenced by high chlorophyll *a* concentration in the hypolimnion ($\sim 10\ \mu g \cdot L^{-1}$) during late summer and autumn, in combination with a completely anoxic hypolimnion ($< 1\ mg \cdot L^{-1}$). It has been reported that productivity and high phytoplankton biomass enhance methanogenesis in freshwater systems (West et al. 2016; West et al. 2015). Bloom frequency and duration are increasing due to climate change, as well as anoxia duration in hypolimnion (Woolway et al. 2021; Jenny et al. 2016) which could enhance methanogenesis rates.

Impacts of future hydrological changes on hypolimnetic metabolism

In the Mediterranean region, severe hydrological changes are expected as a consequence of an increase in extreme drought events and a decrease in runoff and precipitation projected for this area (IPCC 2021). Actually, autumn rainfall in the Iberian Peninsula has already diminished in the last half century as a result of climate change (De Luis et al. 2009), and overall precipitation is expected to decrease in the future for this area (Sumner et al. 2003; Giorgi and Lionello 2008). This could affect stratification periods. Predicted changes in thermal regime as a result of climate change and human pressures will lead to longer thermal stratification and anoxia periods (Woolway and Merchant 2019; Woolway et al. 2021; Jenny et al. 2016). Although the limited hydrological variability included in our study makes any extrapolation to future conditions speculative, future stratification periods could be expected to be similar to that recorded in El Gergal reservoir during 2019 enhancing organic matter oxidation through anaerobic metabolic pathways.

DIC production through some anaerobic pathways (metal reduction, sulfate reduction and methanogenesis) was limited by time since their electron acceptors did not seem to limit their activity in El Gergal. This results in a higher amount of organic matter oxidation by alternative terminal electron pathways when stratification length is extended. Thus, longer anoxia in the hypolimnion leads to higher accumulation of reduced substances Fe^{2+}, Mn^{2+}, NH^{4+}, HS^- which impair water quality (Beutel 2003; Lovley et al. 2004) and increase the cost of drinking water treatment (Verner 1984). In addition, increased anaerobic respiration processes also enhance methanogenesis and, therefore, methane accumulation in the hypolimnion which eventually will be released to the atmosphere after fall turnover.

Nonetheless, hydrology in reservoir ecosystems is human managed, and this can significantly influence water column thermal structure (Casamitjana et al. 2003; Moreno-Ostos et al. 2008) and, therefore, modify the stratification pattern (Wang et al. 2012; Naselli-Flores and Barone 2005). In spite of rainfall differences, water management strategies applied to El Gergal reservoir were different in the two studied years.

In 2019, water inputs and outputs were negligible, allowing greater stability and residence time. By contrast, in 2018, a greater frequency and volume of water inputs from upstream reservoirs and selected withdrawals caused water column instability at the end of summer. Water-level fluctuations due to management strategy and selected withdrawals inducing instability could be used to promote earlier turnover and mixing to reduce both the accumulation of reduced compounds, such as H_2S and dissolved metals, and the reservoir carbon footprint, by reducing CH_4 production.

Supplementary Information The online version contains supplementary material available at https://doi.org/10.1007/s00027-022-00867-2.

Acknowledgements The authors wish to acknowledge the technical staff from Servicio Central de Apoyo a la Investigación (SCAI) of University of Málaga and EMASESA staff for essential technical support during field surveys.

Funding This research was funded by project Alter-C (PID2020-114024GB-C31, PID2020-114024GB-C32, PID2020-114024GB-C33) of Spanish Ministry of Science and Innovation (Spanish Research Agency, AEI). JJM-P was supported by a Spanish FPI grant (RE2018-083596). EMASESA staff provide essential technical support during field surveys. R.M. acknowledges funding from Generalitat de Catalunya through the Consolidated Research Group 2017SGR1124 and the CERCA programme. Open Access funding provided thanks to the CRUE-CSIC agreement with Springer Nature. Funding for open access charge: Universidad de Málaga / CBUA.

Data availability The datasets generated during and/or analysed during the current study are available from the corresponding author on reasonable request.

Declarations

Conflict of interest The authors declare that there are no conflict of interest.

Consent to publish All authors have read and approved the final version of the manuscript.

References

Anderson NJ et al (2020) Anthropogenic alteration of nutrient supply increases the global freshwater carbon sink. Sci Adv 6:1–8

Baines SB et al (1994) Why does the relationship between sinking flux and planktonic primary production differ between lakes and oceans? Limnol Oceanogr 39:213–226

Balistrieri LS et al (1992) The cycling of iron and manganese in the water column of lake Sammamish, Washington. Limnol Oceanogr 37:510–528

Bastviken D et al (2011) Freshwater methane emissions offset the continental carbon sink. Science 331(80):50

Bastviken D et al (2008) Fates of methane from different lake habitats: connecting whole-lake budgets and CH_4 emissions. J Geophys Res Biogeosci 113

Beaulieu JJ et al (2014) Denitrification alternates between a source and sink of nitrous oxide in the hypolimnion of a thermally stratified reservoir. Limnol Oceanogr 59:495–506

Beutel MW (2003) Hypolimnetic anoxia and sediment oxygen demand in california drinking water reservoirs. Lake Reserv Manag 19:208–221

Borges AV et al (2015) Globally significant greenhouse-gas emissions from African inland waters. Nat Geosci 8:637–642

Burns NM et al (2005) Trends in temperature, secchi depth, and dissolved oxygen depletion rates in the central basin of Lake Erie, 1983–2002. J Great Lakes Res 31:35–49

Butcher JB et al (2015) Sensitivity of lake thermal and mixing dynamics to climate change. Clim Change 129:295–305

Canfield ED et al. (2005) Iron and manganese cycles. Aquatic Geomicrobiol 269–311

Cantin A et al (2011) Effects of thermocline deepening on lake plankton communities. Can J Fish Aquat Sci 68:260–276

Carey CC et al (2018) Oxygen dynamics control the burial of organic carbon in a eutrophic reservoir. Limnol Oceanogr Lett 3:293–301

Carpenter SR et al (1986) Chlorophyll production, degradation, and sedimentation: Implications for paleolimnology1. Limnol Oceanogr 31:112–124

Casamitjana X et al. (2003) Effects of the water withdrawal in the stratification patterns of a reservoir. Hydrobiologia. Springer, pp 21–28

Chapra S (1997) Surface water-quality modeling. McGraw-Hill, New York

Chmiel HE et al (2016) The role of sediments in the carbon budget of a small boreal lake. Limnol Oceanogr 61:1814–1825

Cole JJ et al (2007) Plumbing the global carbon cycle: integrating inland waters into the terrestrial carbon budget. Ecosystems 10:172–185

Cornett RJ, Rigler FH (1984) Dependence of hypolimnetic oxygen consumption on ambient oxygen concentration: fact or artifact? Water Resour Res 20:823–830

Cruz-Pizarro L et al (2005) Temporal and spatial variations in the quality of water in El gergal reservoir, Seville. Spain Freshw Forum 23:62–77

De Vicente I et al (2005) Temporal and spatial trends in the sedimentation process in a canyon-type reservoir (El Gergal, Seville, Spain). Arch Für Hydrobiol 163:241–257

De Luis M et al (2009) Seasonal precipitation trends in the Mediterranean Iberian Peninsula in second half of 20th century. Int J Climatol 29:1312–1323

Dean WE, Gorham E (1998) Magnitude and significance of carbon burial in lakes, reservoirs, and peatlands. Geology 26:535–538

del Giorgio PA, Williams PJ le B (2005a) Respiration in aquatic ecosystems. Oxford University Press, New York

del Giorgio PA, Williams PJ le B (2005b) Respiration in lakes. Respiration in aquatic ecosystems. Oxford University Press, New York, p 315

Dickson AG, Goyet C. (1994) Handbook of methods for the analysis of the various parameters of the carbon dioxide system in sea water. A. G. Dick. United States

Dokulil MT et al (2021) Increasing maximum lake surface temperature under climate change. Clim Change 165:56

Doubek JP, Carey CC (2017) Catchment, morphometric, and water quality characteristics differ between reservoirs and naturally formed lakes on a latitudinal gradient in the conterminous United States. Inl Waters 7:171–180

Eckert W, Conrad R (2007) Sulfide and methane evolution in the hypolimnion of a subtropical lake: a three-year study. Biogeochemistry 82:67–76

Edwards WJ et al (2005) Hypolimnetic oxygen depletion dynamics in the central basin of Lake Erie. J Great Lakes Res 31:262–271

Encinas-Fernández J et al (2014) Importance of the autumn overturn and anoxic conditions in the hypolimnion for the annual methane emissions from a temperate lake. Env Sci Technol 48:7297–7304

Fahrner S et al (2008) Organic matter mineralisation in the hypolimnion of an eutrophic Maar lake. Aquat Sci 70:225–237

Fenchel T et al (2012) Bacterial biogeochemistry: the ecophysiology of mineral cycling, 3rd edn. Academic Press, USA

Foley B et al (2012) Long-term changes in oxygen depletion in a small temperate lake: Effects of climate change and eutrophication. Freshw Biol 57:278–289

Gelda RK et al (1995) Determination of sediment oxygen demand by direct measurement and by inference from reduced species accumulation. Mar Freshw Res 46:81–88

George G. (2010) The impact of the changing climate on european lakes. Aquatic Ec. George G (Ed). Springer, Netherlands

Giling DP et al (2017) Delving deeper: Metabolic processes in the metalimnion of stratified lakes. Limnol Oceanogr 62:1288–1306

Giorgi F, Lionello P (2008) Climate change projections for the Mediterranean region. Glob Planet Change 63:90–104

Gómez-Gener L et al (2016) Low contribution of internal metabolism to carbon dioxide emissions along lotic and lentic environments of a Mediterranean fluvial network. J Geophys Res Biogeosciences 121:3030–3044

Grantz EM et al (2012) Partitioning whole-lake denitrification using in situ dinitrogen gas accumulation and intact sediment core experiments. Limnol Oceanogr 57:925–935

Hofmann AF et al (2010) AquaEnv: an aquatic acid-base modelling environment in R. Aquat Geochemistry 16:507–546

Holmer M, Storkholm P (2001) Sulphate reduction and sulphur cycling in lake sediments: a review. Freshw Biol 46:431–451

Hounshell AG et al (2021) Whole-ecosystem oxygenation experiments reveal substantially greater hypolimnetic methane concentrations in reservoirs during anoxia. Limnol Oceanogr Lett 6:33–42

Hoyer AB et al (2009) The influence of external perturbations on the functional composition of phytoplankton in a mediterranean reservoir. Hydrobiologia 636:49–64

Huttunen JT et al (2001) Greenhouse Gases in Non-Oxygenated and Artificially Oxygenated Eutrophied Lakes during Winter Stratification. J Environ Qual 30:387–394

IPCC (2021) Climate change 2021: the physical science basis. contribution of working group I to the sixth assessment report of the intergovernmental panel on climate change. Masson-Delmotte V et al. (Eds). Cambridge University Press

Jenny JP et al (2016) Global spread of hypoxia in freshwater ecosystems during the last three centuries is caused by rising local human pressure. Glob Chang Biol 22:1481–1489

Jones JG, Simon BM (1980) Decomposition Processes in the Profundal Region of Blelham Tarn and the Lund Tubes. J Ecol 68:493–512

Karnachuk OV et al (2006) Distribution, diversity, and activity of sulfate-reducing bacteria in the water column in Gek-Gel lake, Azerbaijan. Microbiology 75:82–89

Kastowski M et al (2011) Long-term carbon burial in European lakes: analysis and estimate. Global Biogeochem Cycles 25:1–12

Kelly CA et al (1988) Carbon and electron flow via methanogenesis, SO_4^{2-}, NO_3^-, Fe^{3+}, and Mn^{4+} reduction in the anoxic hypolimnia of three lakes. Arch Für Hydrobiol 31:333–344

Kortelainen P et al (2004) A large carbon pool and small sink in boreal Holocene lake sediments. Glob Chang Biol 10:1648–1653

Ladwig R et al (2021) Lake thermal structure drives interannual variability in summer anoxia dynamics in a eutrophic lake over 37 years. Hydrol Earth Syst Sci 25:1009–1032

LaRowe DE, Van Cappellen P (2011) Degradation of natural organic matter: a thermodynamic analysis. Geochim Cosmochim Acta 75:2030–2042

Liu M et al (2020) Effects of rainfall on thermal stratification and dissolved oxygen in a deep drinking water reservoir. Hydrol Process 34:3387–3399

Lohse L et al (1993) Nitrogen cycling in North Sea sediments—interaction of denitrification and nitrification in offshore and coastal areas. Mar Ecol Prog Ser 101:283–296

Lovley DR et al (2004) Dissimilatory Fe(III) and Mn(IV) reduction. Adv Microb Physiol 49:219–286

Marcé R et al (2010) El Niño Southern oscillation and climate trends impact reservoir water quality. Glob Chang Biol 16:2857–2865

Matthews DA et al (2008) Electron budgets for the hypolimnion of a recovering urban lake, 1989–2004: response to changes in organic carbon deposition and availability of electron acceptors. Limnol Oceanogr 53:743–759

Mattson MD, Likens GE (1993) Redox Reactions of Organic Matter Decomposition in a Soft Water Lake. Biogeochemistry 19:149–172

McClure RP et al (2021) Ecosystem-Scale Oxygen Manipulations Alter Terminal Electron Acceptor Pathways in a Eutrophic Reservoir. Ecosystems 24:1281–1298

Megonigal JP et al (2014) Anaerobic metabolism: linkages to trace gases and aerobic processes, 2nd edn. Elsevier Ltd, Amsterdam

Mendonça R et al (2017) Organic carbon burial in global lakes and reservoirs. Nat Commun 8:1–7

Millero FJ (1995) Thermodynamics of the carbon dioxide system in the oceans. Geochim Cosmochim Acta 59:661–677

Montes-Pérez JJ et al (2022) Spatio-temporal variability of carbon dioxide and methane emissions from a mediterranean reservoir. Limnetica 41:43–60

Moreno-Ostos E et al (2008) Hydraulic management drives heat budgets and temperature trends in a mediterranean reservoir. Int Rev Hydrobiol 93:131–147

Moreno-Ostos E et al (2012) The gulf stream position influences the functional composition of phytoplankton in El Gergal reservoir (Spain). Limnetica 31:251–260

Moreno Ostos E et al (2016) Planktonic metabolism in a mediterranean reservoir during a near-surface cyanobacterial bloom. Limnetica 35:117–130

Moreno-Ostos E et al (2009a) Spatial heterogeneity of cyanobacteria and diatoms in a thermally stratified canyon-shaped reservoir. Int Rev Hydrobiol 94:245–257

Moreno-Ostos E et al (2009b) The influence of wind-induced mixing on the vertical distribution of buoyant and sinking phytoplankton species. Aquat Ecol 43:271–284

Müller B et al (2012) Hypolimnetic oxygen depletion in eutrophic lakes. Env Sci Technol 46:9964–9971

Naselli-Flores L, Barone R (2005) Water-level fluctuations in mediterranean reservoirs: setting a dewatering threshold as a management tool to improve water quality. Hydrobiologia 548:85–99

Nowicki BL (1994) The effect of temperature, oxygen, salinity, and nutrient enrichment on estuarine denitrification rates measured with a modified nitrogen gas flux technique. Estuar Coast Shelf Sci 38:137–156

Peeters F et al (2019) Sediment fluxes rather than oxic methanogenesis explain diffusive CH_4 emissions from lakes and reservoirs. Sci Rep 9:1–10

Rigosi A, Rueda FJ (2012) Hydraulic control of short-term successional changes in the phytoplankton assemblage in stratified reservoirs. Ecol Eng 44:216–226

Schafran GC, Driscoll CT (1987) Comparison of terrestrial and hypolimnetic sediment generation of acid neutralizing capacity for an acidic adirondack lake. Env Sci Technol 21:988–993

Schindler DW et al (1986) Natural sources of acid neutralizing capacity in low alklinity lakes of the precambrian shield. Science 232(80):844–847

Simola H (1981) Sedimentation in a eutrophic stratified lake in S Finland. Ann Bot Fenn 18:22–36

Soares LMV et al (2019) Modelling drought impacts on the hydrodynamics of a tropical water supply reservoir. Inl Waters 9:422–437

Sobek S et al (2009) Organic carbon burial efficiency in lake sediments controlled by oxygen exposure time and sediment source. Limnol Oceanogr 54:2243–2254

Striegl RG et al (2012) Carbon dioxide and methane emissions from the Yukon River system. Global Biogeochem Cycles 26:GB0E05

Stumm W, Morgan JJ. (1996) Oxidation and reduction; equilibria and microbial mediation. Aquatic Chem: Chem Equilibria Rates Nat Waters 425–515

Sumner GN et al (2003) An estimate of the effects of climate change on the rainfall of mediterranean Spain by the late twenty first century. Clim Dyn 20:789–805

Tranvik LJ et al (2009) Lakes and reservoirs as regulators of carbon cycling and climate. Limnol Oceanogr 54:2298–2314

Vachon D et al (2019) Influence of water column stratification and mixing patterns on the fate of methane produced in deep sediments of a small eutrophic lake. Limnol Oceanogr 64:2114–2128

Verner B (1984) Long term effect of hypolimnetic aeration of lakes and reservoirs, with special consideration of drinking water quality and preparation costs. Lake Reserv Manag 1:134–138

Wang S et al (2012) Effects of local climate and hydrological conditions on the thermal regime of a reservoir at tropic of cancer, in Southern China. Water Res 46:2591–2604

Wang WF et al (2020) Climatic and anthropogenic regulation of carbon transport and transformation in a karst river-reservoir system. Sci Total Env 707:135628

Weiss RF (1974) Carbon dioxide in water and seawater: the solubility of a non-ideal gas. Mar Chem 2:203–215

Wendt-Potthoff K et al (2014) Anaerobic metabolism of two hydromorphological similar pre-dams under contrasting nutrient loading (rappbode reservoir system, Germany). Int Rev Hydrobiol 99:350–362

West WE et al (2015) Phytoplankton lipid content influences freshwater lake methanogenesis. Freshw Biol 60:2261–2269

West WE et al (2016) Productivity and depth regulate lake contributions to atmospheric methane. Limnol Oceanogr 61:S51–S61

Wetzel RG (2001) Limnology: lake and river ecosystems, 3rd edn. Academic Press, Amsterdam

Winslow L et al. (2019) rLakeAnalyzer: lake physics tools

Woolway RI, Merchant CJ (2019) Worldwide alteration of lake mixing regimes in response to climate change. Nat Geosci 12:271–276

Woolway RI et al (2021) Phenological shifts in lake stratification under climate change. Nat Commun 12:2318

Yi Y et al (2021) The impacts of reservoirs on the sources and transport of riverine organic carbon in the karst area: a multi-tracer study. Water Res 194:116933

Yuan LL, Jones JR (2020) Modeling hypolimnetic dissolved oxygen depletion using monitoring data. Can J Fish Aquat Sci 77:814–823

Zeebe RE, Wolf-Gladrow D (2001) CO2 in seawater: equilibrium, kinetics, isotopes, vol 65, 1st edn. Elsevier Science

Zhang F et al (2020) Numerical study of the thermal structure of a stratified temperate monomictic drinking water reservoir. J Hydrol Reg Stud 30:100699